PROCEEDINGS, 50th Workshop on Geothermal Reservoir Engineering
Stanford University, Stanford, California, February 10-12, 2025
SGP-TR-229

Predicting the Lifetime of Geothermal Doublets Analytically

Carolin Wallmeier, Phil Vardon, Alexandros Daniilidis

Stevinweg 1, Room 3.16, 2628CN Delft, Netherlands

c.wallmeier@tudelft.nl

Keywords: thermal breakthrough, direct use, Gringarten

ABSTRACT

A direct-use geothermal doublet can deliver low-emission heat for decades. How long exactly it can deliver heat for, is hard to predict. It depends on geological and technical characteristics and on the minimum required temperature of the water that is produced from the subsurface. Production temperature is typically constant for the first years or decades, and begins to decrease once the colder, re-injected water reaches the producer well. This evolution can be calculated numerically when subsurface conditions are well-known, but that is not usually the case. Especially in the planning phase of doublets, when practical experience is not yet available for new locations, this complicates economic projections. Because direct-use geothermal doublets often have high investments costs and narrow profit margins, this uncertainty can hold back permits and investments in a reliable, sustainable source of heat.

It would be useful to be able to quickly estimate production temperature as a function of time for any geological and technical scenario. In this study, we develop a method to provide such an estimate. We combine an analytical calculation of thermal breakthrough time (following Gringarten and Sauty, 1975) with a parameterized equation for production temperature after thermal breakthrough. This allows us to calculate expected system lifetime. The average root mean squared error (RMSE) of our predicted temperature curves is 0.7K. They are returned nearly instantly and allow to analyze and compare temperature evolution and lifetime across large numbers of scenarios.

1. INTRODUCTION

The production of heat and electricity from deep geothermal energy sources is increasing in many regions around the world (Lund and Toth (2021), Gutiérrez-Negrín (2024)). In areas with sedimentary basins and low to medium geothermal gradients, such as the West Netherlands Basin, heating is the main application because it makes better use of the available temperatures. The typical setup is a doublet, which consists of one well for the production of hot water and one well for the re-injection of colder water. Multiple doublets can be installed in the same area to form a larger system.

Decision makers and project planners that want to permit and build new geothermal systems are often faced with a tight economic outlook. Initial costs for exploration and drilling are high, but successful production is uncertain, especially in green field areas. At the same time, break-even times tend to be long because of narrow profit margins. This means that there can be significant financial risks associated with new geothermal projects, slowing down a development that is much-needed for the energy transition.

1.1 Techno-economic assessment of direct-use geothermal doublets

Techno-economic assessment (TEA) aims to predict the economic outcomes of a planned installation, and how it should be built and operated to increase the chances of economic success. The work flow of a TEA consists of three main steps. First, input parameters are defined that describe the scenario to be investigated. These include expected geological properties, the technical doublet setup, and economic conditions. The second step is the calculation or estimation of key physical variables such as production temperature, required pumping power, and produced heating power. Thirdly, economic indicators are calculated based on these results and the economic input parameters. Examples are net-present value (NPV) and levelized cost of heat (LCOH). The three steps can be run multiple times in order to compare different development scenarios (Daniilidis et al., 2020, Lowry et al., 2021), find optimal operational strategies (Willems and Nick, 2019, Zaal et al., 2021), or understand the effects of uncertainty (Daniilidis et al., 2017, Gkousis et al., 2024).

1.2 Goal of this study

Because geothermal heating systems are long-term projects that only pay off over decades, a prediction of how production temperature T_{Prd} will develop over time is an important component of a TEA. The amount of produced thermal power that can be sold is one of the most important variables for any economic indicator, and directly proportional to the thermal energy that can be extracted from the produced water.

While a number of TEA tools for deep geothermal energy have been published, to our knowledge none of them are aimed at heat production from porous reservoirs and also include the transient aspect of $T_{Prd}(t)$. Beckers and McCabe (2019) summarize that some tools were made for electricity production from fractured rocks, such as GETEM (US DOE 2016), HDRec (Heidinger et al. 2006) and Euronaut (Heidinger 2010). DoubletCalc (Mijnlieff et al., 2014) is aimed at heating applications and includes detailed calculations of pressure and heat developments in the system, but assumes steady state conditions. GEOPHIRES2 (Beckers and McCabe, 2019) includes models for electricity as well as heat, and also for temperature decline. However, in the heating mode, $T_{Prd}(t)$ is approximated with a linear decline,

the slope of which has to be specified by the user. Alternatively, a pre-calculated temperature profile can be input or calculated by TOUGH2 on the fly, but this requires time-consuming numerical simulations.

The main goal of this study was to build the physics component of a TEA model for geothermal heating doublets. It should be fast and reliable for a large range of geological and operational parameters. What distinguishes it from existing efforts is the ability to predict production temperature evolution and, given a minimum acceptable production temperature T_{Min}, system lifetime.

2. THE MODEL

The model input is a doublet scenario, described by the geological and technical parameters listed in Table 1. It provides four key outputs that can be used in a TEA: 1) The pressure difference Δp between the two wells which has to be overcome by pumps, 2) The time of thermal breakthrough after which temperature starts to decline, 3) Transient production temperature $T_{Prd}(t)$, and 4) expected system lifetime for a minimum acceptable production temperature T_{Min}.

Δp and t_{BT} can be obtained analytically using the assumptions made by Gringarten and Sauty (1975). The temperature evolution after breakthrough is more complex, which is why it is usually omitted or approximated as a simple decline function. To be able to predict it more accurately, we carried out numerical simulations of a large number of doublet setups that varied in seven key parameters (bold rows in Table 1). We fitted the observed temperature profiles with functions of the type

$$T_{Prd}(t) = T_{Inj} + \left(\frac{\Delta T_{Max}}{ln\left(e + \left(\frac{t}{t_{BT}}\right)^{n}\right)}\right)^{m} \tag{1.1}$$

Where T_{Inj} is the re-injection temperature and ΔT_{Max} is the difference between initial production temperature T_0 and T_{Inj}. We built an interpolator that provides estimates of the coefficients m and n for any new combination of parameters. Eq. (1.1) was chosen out of candidates including logistic, polynomial and rational functions because it provided the best fits with only two unknown coefficients.

Table 1: Input parameters for the Doublet model. Bold parameters were varied and enter into the prediction of $T_{Prd}(t)$ coefficients.

Component	Parameter	Unit	Description	Range / Value
Physics - Geology	**d**	**m**	**Top depth of the reservoir**	**1500 – 2500**
Physics - Geology	**h**	**m**	**Height of the reservoir**	**20 – 100**
Physics - Geology	**φ**	**fraction of 1**	**Rock porosity**	**0.1 – 0.2**
Physics - Geology	**k**	**mD**	**Rock permeability**	**150 – 450**
Physics - Geology	**α_{conf}**	**W/(mK)**	**Confining layer thermal conductivity**	**2 – 3**
Physics - Geology	ρ_R	kg/m^3	Rock density	2300
Physics - Geology	Cp_R	J/(kgK)	Rock heat capacity	1000
Physics - Geology	T_{surf}	°C	Surface temperature	10
Physics - Geology	T_{grad}	K/m	Temperature gradient	0.03
Physics - Technical	**L**	**m**	**Well spacing**	**400 – 1200**
Physics - Technical	**q**	**m^3/h**	**Flow rate**	**150 – 450**
Physics - Technical	**T_{Inj}**	**°C**	**Injection temperature**	**20 – 50**
Physics - Technical	r_{Well}	m	Well radius	0.1016

The Gringarten assumptions used for Δp and t_{BT} are:

1. The reservoir is homogeneous, horizontal, and isotropic.

2. The fluid flow is Darcy flow.

3. The fluid and the rock matrix are in local thermal equilibrium everywhere.

4. There are no confining layers.

5. There is no horizontal conduction of heat.

6. Vertical heat conduction is infinite, so $T(z)$ in the reservoir is constant.

We used the reservoir simulator DARTS (open Delft Advanced Research Terra Simulator, Voskov et al., (2025)) to validate these results by comparing them with two versions of DARTS models: In one, all six Gringarten assumptions are implemented to test the match between the analytical and numerical computation of the same equations and boundary conditions. In the other, only assumptions 1-3 are implemented. There are confining layers with varied thermal conductivity, as well as a fixed thermal conductivity of 3W/mK in the reservoir. This allows to test the validity of the assumptions and their impact on calculated Δp and t_{BT}. In the following, the two versions are referred to as DARTS-Ana and DARTS-Full, respectively.

For the temperature curves that informed the interpolator, we used DARTS-Full models. While the presence or absence of confining layers does not significantly influence time of thermal breakthrough (Fig. 2, de Bruijn et al., 2021), it slows down the decline in T_{Prd} afterwards (Wang et al., 2021), so models without confining layers would be unrealistically pessimistic.

The choice of boundary conditions and grid resolution follows the approach outlined in Chen et al. (2025). All models are 3km wide and 3km + well spacing L long. They have a horizontal resolution of 10m in the inner zone around the doublet, and up to 50m near the edges (Fig. 1a). Vertical resolution is 2m in the reservoir and confining layers, where existing, are 300m thick with a vertical resolution graded from 2 – 50m.

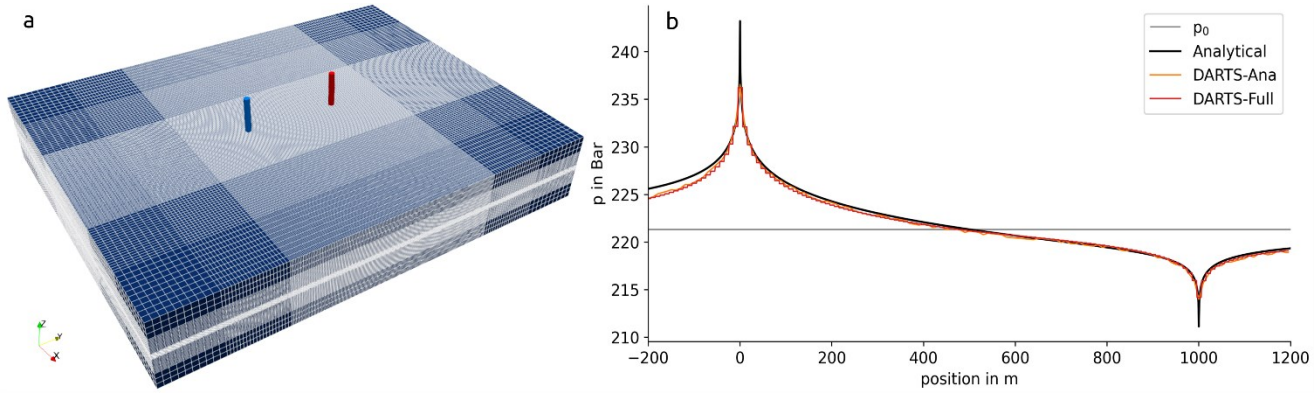

Figure 1. a) DARTS-Full model domain, here L = 1000m, d = 2200m, h = 100m, q = 200m³/h and T_{Inj} = 30°C. Producer and injector wells in red and blue, respectively. b) Pressure profiles along a doublet plane cross section. Analytical vs. DARTS-Ana (no confining layers) and DARTS-Full (confining layers).

2.1 Pressure

The initial pressure at the mid-depth of the reservoir is

$$p_0 = p_{surf} + (d + \frac{h}{2})\frac{dp}{dz}, \tag{1.2}$$

where p_{surf} is the average surface pressure, d is the depth of the top of the reservoir, h is the height of the reservoir and dp/dz is the hydrostatic gradient. We assume that, under rate-controlled wells, a new steady-state pressure distribution is reached quickly after production begins. At any point in the reservoir, it is the sum of a pressure high around the injector and a pressure-low around the producer. For a point x between the two wells - where x is the distance from the injector and $(L - x)$ is the distance from the producer - these effects can be expressed as

$$dp_{Inj}(x) = \frac{\mu(x)}{k}\frac{q}{2\pi h} ln(\frac{x_\infty}{x}) \tag{1.3}$$

and

$$dp_{Prd}(x) = -\frac{\mu(x)}{k}\frac{q}{2\pi h} ln(\frac{x_\infty}{L-x}) \tag{1.4}$$

where $\mu(x)$ is the water viscosity at point x, assuming that it varies linearly between the end-values associated with T_{Inj} and T_0. x_∞ is a point so far away from the doublet that it is unaffected by pressure changes. The absolute pressure at point x is then

$$p(x) = p_0 + \mu(x)\frac{q}{2\pi hk} ln(\frac{L-x}{x}) \tag{1.5}$$

and the pressure drop Δp that has to be overcome by pumping is

$$\Delta p = p(0) - p(L) \approx p(r_{Well}) - p(L - r_{Well}) = \frac{(\mu_{Inj} + \mu_{Prd})}{2}\frac{q}{\pi hk} ln(\frac{L - r_{well}}{r_{well}}). \tag{1.6}$$

For pressure at the wells, 0 and L are substituted with r_{Well} and $(L - r_{Well})$ because eq. (1.6) is undefined for $x = 0$ and $x = L$, and because the pressure regime inside the wells is different from that in the reservoir.

Fig. 1b shows the analytical pressure profile for a doublet with 1km well spacing. The same curve extracted from two DARTS-Ana and DARTS-Full is plotted for comparison. The match between all three is very close, except in the direct vicinity of the wells. This is because the Darts solution averages pressure across 10m cells and cannot reflect the peak accurately.

2.1 Time of thermal breakthrough

From the assumptions of Darcy flow and local thermal equilibrium, it follows that the thermal front moves with a velocity proportional to that of the fluid particles.

$$v_{cold} = \frac{\lambda}{\phi} v_{Darcy} \tag{2.1}$$

with

$$\lambda = \frac{\phi \rho c_f}{(1-\phi)\rho_r c_r + \phi \rho_f c_f}. \tag{2.2}$$

The time it takes the cold front to spread from the injector to the producer is given by the integral of its velocity along the doublet axis.

$$t_{BT} = \frac{\phi}{\lambda}\frac{\pi h L^2}{3q}. \tag{2.3}$$

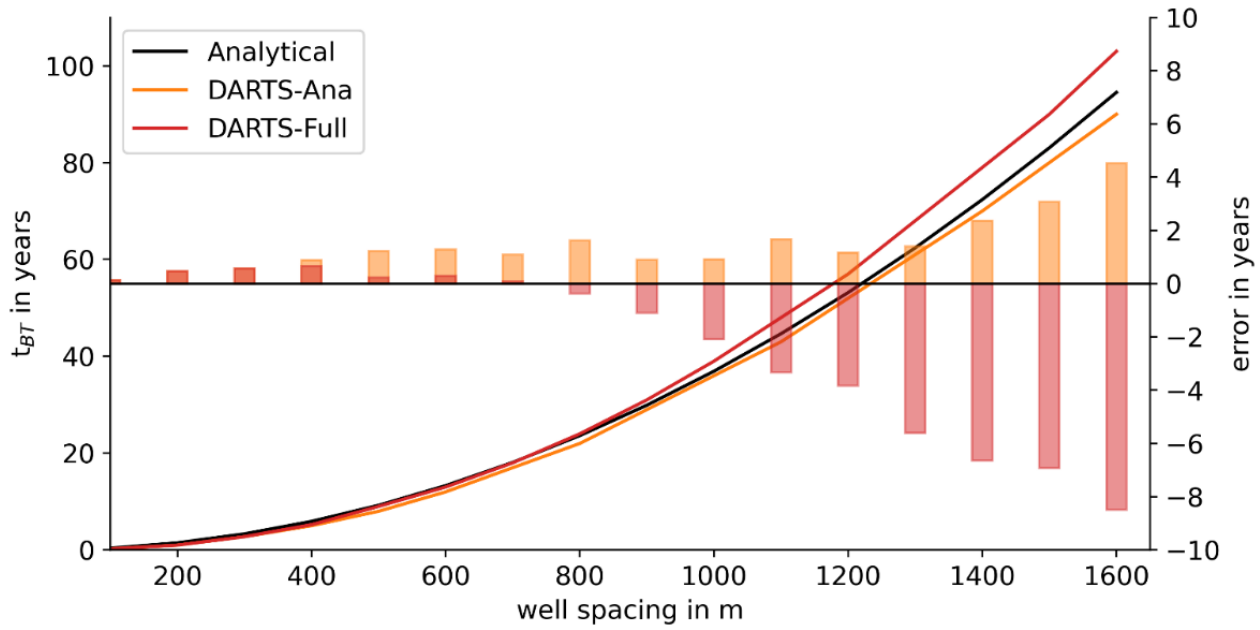

Figure 2. Time of thermal breakthrough (T_{BT}) calculated for different well spacings. Analytical solution compared with DARTS-Ana (no confining layers) and DARTS-Full (confining layers).

This is the analytical solution for cold front propagation published by Gringarten and Sauty (1975), in the version that assumes no heat transfer between reservoir and confining layers. For numerical validation, we simulated different doublets with a range of well spacings and monitored production temperature. We defined time of thermal breakthrough as the year in which T_{Prd} drops below its initial value by 0.1K. The solutions match up to well spacings above 1000m, where the error introduced by this assumptions becomes noticeable (Fig. 2). Time of breakthrough for a spacing of 1600m is estimated as 94 years, compared to ca. 102 years in the full Darts solution.

Gringarten and Sauty also provide a parameter (referred to as λ or k) that can be added to the equation to describe this heat exchange and make temperature predictions more accurate. It is relevant especially when the Gringarten solution is used to calculate T_{Prd} after breakthrough. Pogacnik et al. (2023), however, showed that it has to be increased above its physical value, by an order of magnitude in some cases, to achieve an optimal fit with trusted numerical solutions. Given the good results for time of breakthrough, and given that in low-enthalpy heating applications, ΔT_{Max} between production and injection temperature is limited, adding this parameter does not significantly improve our results.

2.3 Transient production temperature

We identified seven geological and technical parameters that control the shape of the temperature decline after thermal breakthrough: Well spacing, reservoir depth and height, injection temperature, flow rate, porosity (and permeability through a fixed correlation), and the thermal conductivity of the confining layers. Thermal conductivity of the reservoir layer has close to no influence on T_{Prd} because advective heat transport is the dominant mechanism there.

In DARTS, we simulated 1458 cases for 100 years each, covering the 7D parameter space (Table 1) in a full factorial design. Three values for each parameter were combined with each other, except confining layer conductivity which received only the two end points. 1319 simulations were completed successfully, the remaining 139 did not converge within the pressure range permitted in DARTS because they described unrealistic setups that lead to extremely low production well pressures. They were omitted from further analysis.

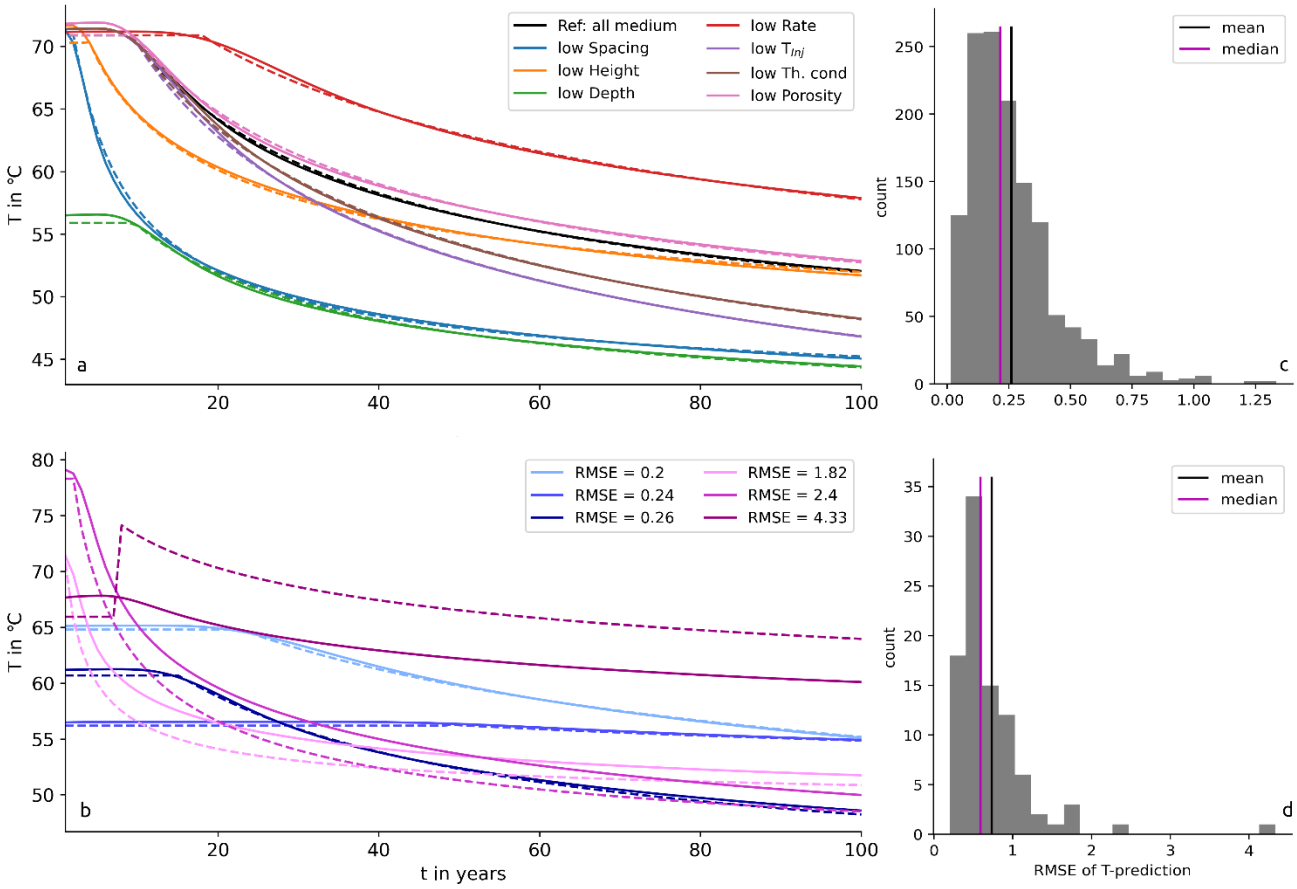

Figure 3. a) Fitted curves from the full factorial setup. Reference with all parameters at medium value and variants with one parameter at lower value each. b) Best and worst three of the testing curves. c) and d) histograms of RMSE for fitted and tested curves, respectively.

We calculated t_{BT} as described above and used scipy's curve_fit (Virtanen et al., 2020) to find the optimal coefficients m and n to make eq. (1.1) match the shape of the observed temperature profile after thermal breakthrough (Fig. 3a). Until t_{BT}, we assume that T_{Prd} equals T_0. This method resulted in better fits than matching the whole profile starting from t=0. The first time step after t_{BT} was given a higher weight than the other time steps, ensuring that the fitted part of the curve started correctly from T_0. A histogram of the root-mean squared

error (RMSE, Fig. 3c) shows that most temperature profiles can be fitted well. The average RMSE is just under 0.2 Kelvin and the distribution is strongly skewed towards small errors. Only 11 cases have an RMSE above 1K. They all describe a deep, thin reservoir with a large L, high q and high T_{Inj}. This leads to a steep but relatively straight temperature decline which is not matched ideally by the chosen curve type.

The observed temperature curves informed a scipy LinearNDInterpolator object which returns the pair (m, n) for any combination of doublet parameters in the input range. We tested the predictive quality of these coefficients with 100 additional doublet setups, randomly distributed across the 7D space, and simulated in DARTS for comparison. Their T_{Prd} profiles are predicted well in many but not all cases. The shape of the RMSE distribution is similar to that for the fitted cases, but higher with an average of 0.7K (Fig. 3d). 15 out of the 100 cases have an RMSE above 1K, with two outliers above 2 and 4K. Fig. 3b shows the predicted and observed temperature curves for the three cases that were predicted with the smallest and largest RMSE, respectively.

Most of the doublet setups that were predicted well show a similar type of T_{Prd} curve. It drops not too early or too late and not too strongly or too weakly. Among the three profiles that were predicted the worst (purple in Fig. 3b) are two with almost an L-shape, a very early and steep decline followed by a relatively flat part. The third is the opposite, a slow but almost constant decline. Both shapes are edge cases that occur only in specific regions of the parameter space. They are also near the "holes" in the interpolator grid that were left by the 139 cases that had to be excluded. The steep decline of the L-shape is the result of high q in deep and relatively thin reservoirs. A high T_{Inj} and small well spacing create the flat part. The third profile that is flat throughout, combines a shallow reservoir with a high T_{Inj}. Its shape is predicted relatively well, but the overall temperature level is wrong because it is highly sensitive to small changes in m.

2.4 System Lifetime

Expected lifetime LT is defined as the first year when predicted T_{Prd} is lower than T_{Min} (Fig. 4). We calculated it for the 100 test cases for three different values of T_{Min} each: 3K, 5K, and 10K below a case's initial temperature T_0. The prediction is good in most cases, especially for the 3K definition and lifetimes below 40 years. Above, the spread increases and there are more outliers. The RMSE is 6.9, 4.1 and 4.9 years for accepted ΔT of 3, 5 and 10K, respectively. Without the one outlier whose temperature profile had been predicted very badly, these errors would be 2.8, 3.1 and 4.9 years. This second set of errors matches better the clearly higher prediction quality for shorter lifetimes.

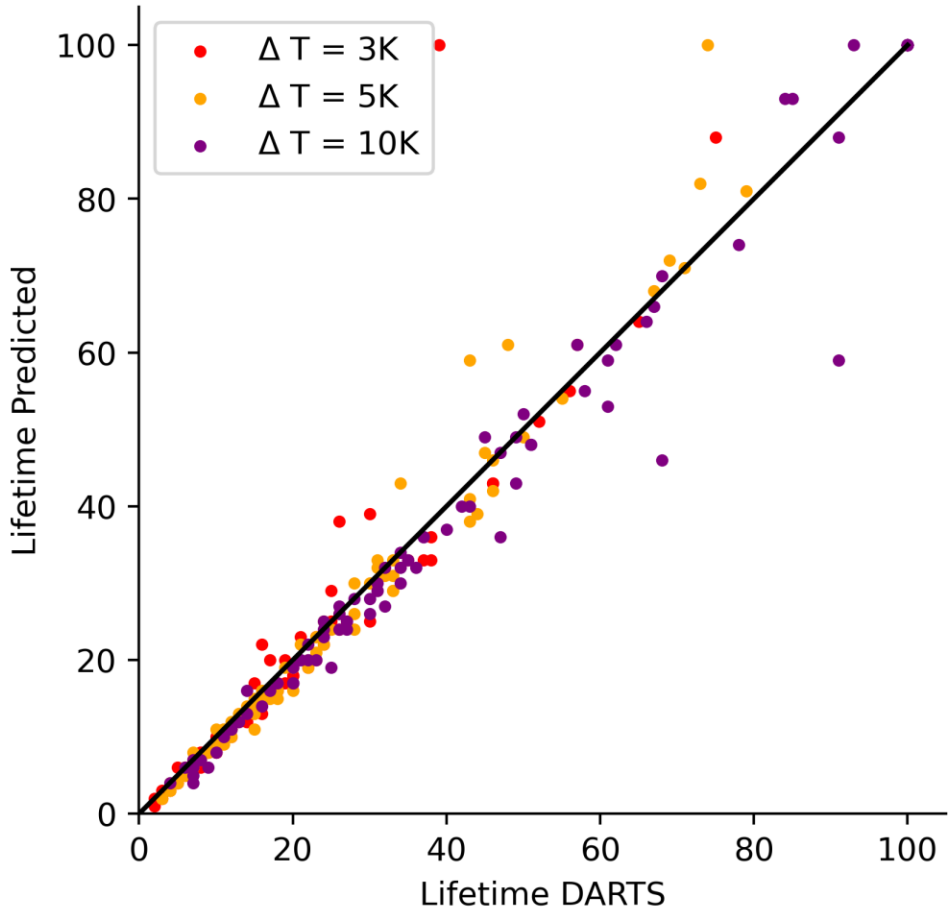

Figure 4 Predicted lifetime vs calculated lifetime from DARTS simulations. Lifetime defined as reaching a T-drop of 3, 5 and 10K.

3. CONCLUSIONS

We have predicted production temperature $T_{Prd}(t)$ and lifetime LT for a wide range of direct use geothermal doublet setups. From numerical simulations using DARTS, we sampled $T_{Prd}(t)$ on a full factorial grid across seven geological and technical parameters and fitted it with an equation that uses analytically calculated time of thermal breakthrough t_{BT} and maximum temperature drop $\Delta T_{Max,}$, as well as two coefficients m and n. We showed that linear interpolation of m and n on a 7D grid allows to predict $T_{Prd}(t)$ for new combinations in the parameter range with a mean RMSE of 0.7K. For Doublets near the middle of the space, the error was lower, while combinations with particularly steep or particularly flat temperature curves were predicted less well. This is encouraging because most realistic doublet setups were predicted well. The ones with larger errors tend to represent scenarios unlikely to be planned in reality, such as combining a shallow reservoir with a high T_{Inj} which results in a ΔT of only a few degrees, or pumping a very high flowrate through a shallow reservoir with small well spacing, resulting in extremely fast cooling. Given that each parameter was only sampled with three values and that about 10% of the interpolation grid was unfilled, the fit could most likely be improved by filling the grid holes and making it denser.

However, in a 7D parameter space, sampling even just one additional point on each axis would increase the number of required cases almost tenfold. In following research, we will therefore focus on approaches to improve predictive quality without exponentially increasing the number of training simulations. We will adjust the resolution of the parameter space based on which dimensions and regions are more or less sensitive to changes, and we will investigate the relationships between the doublet parameters and the two coefficients.

REFERENCES

Chen, Y., Voskov, D., Daniilidis, A., (2025). Rigorous Numerical Methodology and Heat Recovery Analysis for Modeling of Direct Use Geothermal Systems. Geoenergy Science and Engineering 247, 213661.

Daniilidis, A., Alpsoy, B., Herber, R., (2017). Impact of technical and economic uncertainties on the economic performance of a deep geothermal heat system. Renewable Energy 114, 805–816.

Daniilidis, A., Nick, H.M., Bruhn, D.F., (2020). Interdependencies between physical, design and operational parameters for direct use geothermal heat in faulted hydrothermal reservoirs. Geothermics 86, 101806.

De Bruijn, E.A.M., Bloemendal, M., ter Borgh, M.M., Godderij, R.R.G.G., Vossepoel, F.C., (2021). Quantifying the contribution of heat recharge from confining layers to geothermal resources. Geothermics 93, 102072.

Gutiérrez-Negrín, L.C.A. Evolution of worldwide geothermal power 2020–2023. Geotherm Energy 12, 14 (2024)

Gkousis, S., Welkenhuysen, K., Compernolle, T., (2024). Integrated assessment of deep geothermal heating investments in Northern Belgium through techno-economic, life cycle, global sensitivity and real options analysis. Geothermics 121, 103027.

Lowry, T., Sabin, A., Ayling, B., Hinz, N., Tiedeman, A., Arguello, R., Blake, K., (2021). Deep Direct-Use Geothermal: A Probabilistic Systems Analysis Approach for Techno-Economic Analysis.

Lund, J. W., Toth, A. N. (2021) Direct utilization of geothermal energy 2020 worldwide review, Geothermics 90, 101915

Pogacnik, J., Harcouët-Menou, V., Laenen, B., (2023). Analytical Estimation for the Production Temperature of a Geothermal Doublet.

Voskov, D., Saifullin, I., Wapperom, M., Tian, X., Palha, A., Orozco, L., & Novikov, A. (2025). Open Delft Advanced Research Terra Simulator (open-DARTS) (1.2.2). Zenodo

Wang, Y., Voskov, D., Khait, M., Saeid, S., Bruhn, D., 2021. Influential factors on the development of a low-enthalpy geothermal reservoir: A sensitivity study of a realistic field. Renewable Energy 179, 641–651.

Willems, C.J.L., Nick, H.M., (2019). Towards optimisation of geothermal heat recovery: An example from the West Netherlands Basin. Applied Energy 247, 582–593.

Zaal, C., Daniilidis, A., Vossepoel, F.C., (2021). Economic and fault stability analysis of geothermal field development in direct-use hydrothermal reservoirs. Geothermal Energy 9, 12.